Longitudinal variations of electron temperature and total ion density in the sunset equatorial topside ionosphere

Zhipeng Ren,[1,2,3] Weixing Wan,[1] Libo Liu,[1] Biqiang Zhao,[1] Yong Wei,[1,2,3] Xinan Yue,[1,2,3] and Roderick A. Heelis[4]

Received 13 December 2007; revised 15 January 2008; accepted 31 January 2008; published 15 March 2008.

[1] Based on the DMSP F13 Satellite observations from 1995 to 2005, the longitudinal distributions of the electron temperature (T_e) and total ion density (N_i) in the sunset equatorial topside ionosphere are examined. The results suggest that the longitudinal variations of both T_e and N_i exhibit obvious seasonal dependence as follows: (1) wavenumber-four longitudinal structure in equinox, (2) three peaks structure in June solstice, and (3) two peaks structure in December solstice. Moreover, the longitudinal variations of T_e and N_i show significant anti-correlation, and we speculate that the longitudinal variation of T_e may result from that of N_i which can control T_e through the electron cooling rate. The wavenumber-four longitudinal structures of both T_e and N_i in equinox may relate to the eastward propagating zonal wavenumber-3 diurnal tide (DE3), which has effect on the amplitude of the daytime zonal electric field. The longitudinal variation of T_e and N_i in the two solstices may be caused both by longitudinal variation of geomagnetic declination and DE3. **Citation:** Ren, Z., W. Wan, L. Liu, B. Zhao, Y. Wei, X. Yue, and R. A. Heelis (2008), Longitudinal variations of electron temperature and total ion density in the sunset equatorial topside ionosphere, *Geophys. Res. Lett.*, *35*, L05108, doi:10.1029/2007GL032998.

1. Introduction

[2] The low-latitude ionosphere is a highly dynamic environment that exhibits significant variations with local time, altitude, latitude, longitude, solar cycle, season, and geomagnetic activity. Recently, using the nightglow images of OI 135.6-nm from the Far Ultraviolet imager (FUV) on board the Imager for Magnetopause-to-Aurora Global Exploration (IMAGE) and the Global Ultraviolet Imager (GUVI) on board the Thermosphere Ionosphere Mesosphere Energetics and Dynamics (TIMED) satellites, *Sagawa et al.* [2005] and *Henderson et al.* [2005] individually demonstrated the global wavenumber-four longitudinal structure in the amplitude and separation of the nighttime equatorial ionization anomaly (EIA). More recently, *England et al.* [2006a] found that this nighttime wavenumber-four structure is absent during solstice periods in the nighttime UV observations. *Lin et al.* [2007a, 2007b] analyzed the electron density profiles and the diurnal variation of the wavenumber-4 patterns. Using the long duration TEC data measured by the TOPEX/Poseidon altimeter, *Scherliess et al.* [2008] found that the wavenumber-four longitudinal structure undergo a remarkable seasonal variation. W. Wan et al. (Wavenumber-4 patterns of the total electron content over the low latitude ionosphere, submitted to *Geophysical Research Letters*, 2007) studied in detail the diurnal seasonal and solar cycle variations of this longitudinal structure. *Immel et al.* [2006] found the peak locations of this longitudinal structure with the coincidence of the peak locations of the tidal amplitude predicted by the Global Scale Wave Model (GSWM) [*Hagan and Forbes*, 2002] and explained this structure as the effects of longitudinal variations in the amplitude of atmospheric tides in the daytime ionospheric E region and the corresponding modulation of the daytime zonal electric field [see also *England et al.*, 2006b; *Hartman and Heelis.*, 2007; *Kil et al.*, 2007; *Hagan et al.*, 2007].

[3] The previous studies have shown that the ionospheric variations have significant altitude dependencies and the behaviors in the topside ionosphere are rather different from those at the peak of F2 layer [e.g., *Balan et al.*, 1997; *Liu et al.*, 2007a, 2007b; *Rich et al.*, 2003; *Rishbeth et al.*, 1977; *Venkatraman and Heelis*, 1999a, 1999b, 2000; *Zhao et al.*, 2005]. Many researchers suggest that the topside ionosphere electron temperature (referred to as T_e) and plasma density (referred to as N_i) undergoes a strong longitude effect [e.g., *Liu et al.*, 2007a; *Su et al.*, 1996; *Venkatraman and Heelis*, 1999a, 2000]. Because of the near-horizontal magnetic field and related electrodynamics process, the equatorial ionosphere has unique features. Particularly, a stronger fountain effect can enhance N_i at anomaly latitudes but reduces it at the dip equator, so the longitudinal variation at the dip equator may show some interesting characteristics. Recently, *Hartman and Heelis* [2007] and *Kil et al.* [2007] individually found a wavenumber-four structure in the daytime vertical $\mathbf{E} \times \mathbf{B}$ drift velocity which can affect the longitudinal variation in the topside ionosphere. In this paper, we use observations of T_e and total ion density (N_i) from Defense Meteorological Satellite Program (DMSP) F13 satellite over a total of 11 years (from 1995 to 2005) to investigate the longitudinal and seasonal variations of T_e and N_i in the sunset equatorial topside ionosphere. The DMSP satellites, whose orbital planes' local time is nearly constant at middle and low latitudes, provide long term observations of thermal plasma

[1]Institute of Geology and Geophysics, Chinese Academy of Sciences, Beijing, China.
[2]Wuhan Institute of Physics and Mathematics, Chinese Academy of Sciences, Wuhan, China.
[3]Graduate School, Chinese Academy of Sciences, Beijing, China.
[4]Hanson Center for Space Sciences, University of Texas at Dallas, Richardson, Texas, USA.

0094-8276/08/2007GL032998$05.00

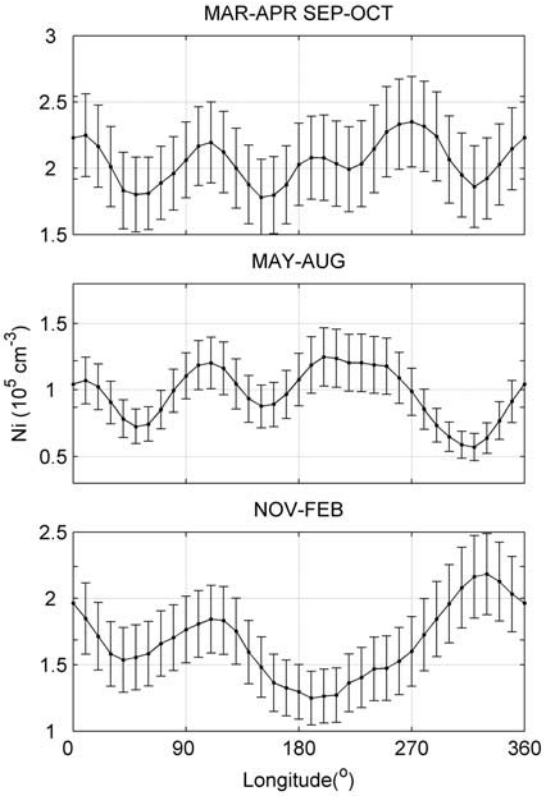

Figure 1. Longitudinal variations of quiet time average N_i in different seasons. See the text for details. The vertical bars indicate the scatter on the satellite data. In order to show the detail of the longitudinal variation in this figure, the vertical bars are reduced to its 20%.

in the topside ionosphere, which allow a rather complete description of longitude and seasonal variations.

2. Observations

[4] The series of the DMSP spacecrafts, which are designated with the letter F and the flight number, e.g., F13, are in sun-synchronous polar orbits. The average altitude of F13 over the geographical equator over its lifetime is ~850 km. The orbital inclination of F13 is 98.8°. The period of an orbit is about 101 minutes, and consecutive orbits are separated in longitude by 25.5°. The spacecraft carries a "Special Sensor-Ions, Electrons and Scintillation" (SSIES) package to monitor the behavior of thermal plasma in the topside ionosphere since 1987. The T_e is measured with the onboard Langmuir probe, and the N_i is measured with the onboard scintillation meter. In this paper, data in the sunset (the average local time is 1745) sectors from the spacecraft F13 were chosen for analysis. The T_e and N_i data are provided at the University of Texas, Dallas (UTD) Web site (http://cindispace.utdallas.edu/DMSP/) with 4-s resolution. Only the data whose location's dip angle is between ±2° have been used in our work. We determined the dip angle using the International Geomagnetic Reference Field (IGRF) model for the appropriate epoch. The Observations taken during periods of high magnetic activity marked by the $K_p > 3$ were removed from the data set in order to confine our attention to quiet conditions. Due to the season-dependence of longitudinal variation of T_e and N_i, we separate the T_e and N_i data according to the season. In detail, the data were separated into three 4-month long seasonal bins: Equinox (March–April, September–October), June solstice (May–August), and December solstice (November–February). Then we binned them every 10° in longitude into 36 geographical longitude bins which are all 30° wild. Finally, in each bin the mean values were calculated.

[5] Figure 1 shows the longitudinal variation of quiet time average N_i in different seasons. The vertical bars indicate the scatter on the satellite data. This scatter mainly relate to the solar cycle variation of N_i [see *Zhao et al.*, 2005]. However, as we use 11 years' DMSP data in this research, the solar cycle variation of N_i is much stronger than longitudinal variation of N_i. To show the detail of the longitudinal variation in Figure 1, the vertical bars are reduced to 20%. There is a manifest wavenumber-four longitudinal structure for the equinox conditions with maxima located at near 10°E, 110°E, 200°E, and 270°E longitude. Figure 1 also shows a notable three peaks longitudinal structure for the June solstice conditions with maxima located at near 10°E, 110°E, and 200°E longitude, and a two peaks longitudinal structure during December solstice conditions with maxima located at near 110°E and 320°E longitude. The longitudinal variations of quiet time average T_e in different seasons are plotted in Figure 2. The vertical bars indicate the scatter on the satellite data. To show the detail of the longitudinal variation in Figure 2, the vertical

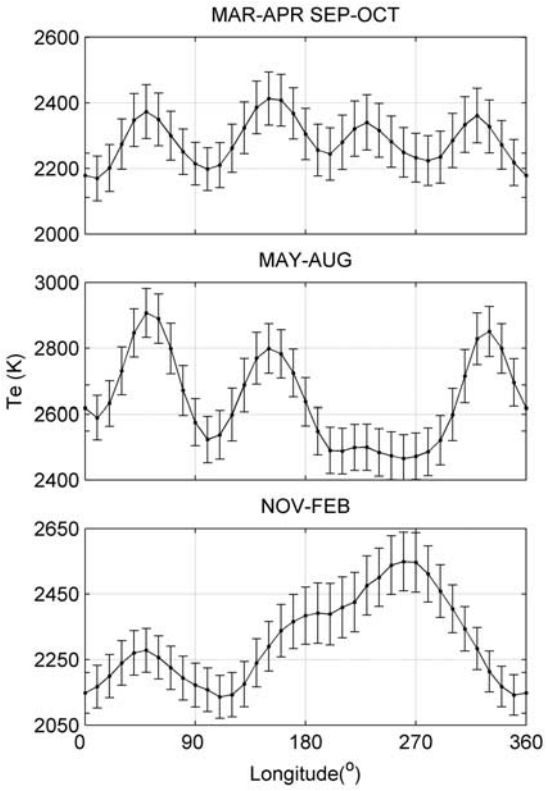

Figure 2. Longitudinal variations of quiet time average T_e in different seasons. See the text for details. The vertical bars indicate the scatter on the satellite data. In order to show the detail of the longitudinal variation in this figure, the vertical bars are reduced to its 20%.

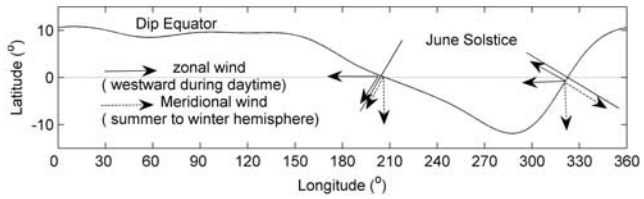

Figure 3. Effects of the meridional and zonal winds when their components along the magnetic field lines are constructive near the dip equator during the June solstice. Note that the lengths of the arrows for the two winds are chosen for illustration purpose only and do not represent their relative magnitude.

bars are also reduced to 20%. Among these three seasons, the longitudinal variation near the equinox is weakest. The longitudinal variation of quiet time average T_e also show wavenumber-four longitudinal structure in equinox, three peaks structure in June solstice, and two peaks structure in December solstice. However, the longitudinal variations of T_e are almost opposite that of N_i in all seasons, and the maxima of T_e mainly locate near the minima of N_i, the minima of T_e mainly locate near the maxima of N_i.

3. Discussion and Conclusions

[6] It is well known that the ionospheric electron temperature depends on electron density and the neutral atmosphere (see *Schunk and Nagy* [1978] and *Lei et al.* [2007] for details). In the topside ionosphere, the electron heating rate is proportional to electron density, and the electron cooling rate, which mainly relates to Coulomb collisions with the ions, is proportional to the square of electron density. The competing process between the electron heating rate and the electron cooling rate determines the variation of the electron temperature [see *Otsuka et al.*, 1998]. In fact, the anti-correlations between electron temperature and electron density are widely applied to develop empirical electron temperature models [e.g., *Bilitza*, 1975]. As seen from a comparison of Figures 1 and 2, the longitudinal variation of T_e is almost opposite that of N_i in all seasons, which is expected from the anti-correlation between T_e and N_i [*Schunk and Nagy*, 1978]. T_e increases when N_i decreases and T_e decreases when N_i increases. Thus, the longitudinal variation of T_e mainly relates to the longitudinal variation of N_i which can control T_e through the electron cooling rate. However, T_e increases when N_i increases in the region between 180°E and 270°E for the December solstice conditions. We should notice that the geomagnetic field declination, which can also influence the plasma temperatures near the equator through the action of wind induced plasma transport along the geomagnetic field lines, reaches its positive (eastward) maxima in the region between 180°E and 270°E. Thus, the abnormity between 180°E and 270°E during the December solstice may related to the transequatorial winds which can drive the plasma along geomagnetic field lines [see also *Venkatraman and Heelis*, 1999a].

[7] Similarly to the longitude distribution of N_i during equinox periods near 1745 LT, a global wavenumber-four longitudinal structure in the equinox nighttime EIA have also been found by *Sagawa et al.* [2005] and *Henderson et al.* [2005], respectively. The EIA, which is closely associated with the upward vertical plasma drifts, is an important feature of the low-latitude ionosphere. During the daytime, the E-region dynamo, which is driven by neutral wind, produces an eastward electric field near the magnetic equator. These electric fields, which are transmitted upward along magnetic field lines into the F-region, cause the uplift of ionospheric plasma at the magnetic equator to altitudes >800 km. Then, through diffusion and gravitational sedimentation, the upward lifted plasma settles along the magnetic field to locations north and south of the equator and forms the equatorial anomaly. Although a stronger fountain effect mainly enhances N_i at anomaly latitudes but reduces it at the dip equator, the upward vertical plasma $\mathbf{E} \times \mathbf{B}$ drifts will also increase N_i in the topside ionosphere (>800 km) where the EIA disappear. Thus, the wave number-four longitudinal structure in equinox topside ionospheric N_i is closely associated with the wave number-four longitudinal structure in the equinox nighttime EIA. *Immel et al.* [2006] explained the observed nighttime longitudinal structure of the EIA as the result of longitudinal variations in the diurnal amplitude of atmospheric tides in the daytime E region ionosphere and a corresponding modulation of the daytime zonal electric field. Based on a series of simulations with TIME-GCM, *Hagan et al.* [2007] proved that the wavenumber-four longitudinal structure in the equinox nighttime EIA can be explained by the effects of an eastward propagating zonal wavenumber-3 diurnal tide (DE3) that is excited by latent heat release associated with raindrop formation in the tropical troposphere [see also *Hagan and Forbes*, 2002]. With the effect of DE3, the meridional winds at E region will exhibit four maxima. At the locations of the four peaks, the meridional winds may enhance the Pedersen currents in the E-region, strengthening the daytime eastward electric field and thus produced a stronger equatorial plasma fountain [e.g., *England et al.*, 2006b; *Hartman and Heelis*, 2007; *Kil et al.*, 2007]. The stronger equatorial plasma fountain then results in the stronger N_i in the four regions of the topside ionosphere. Near the locations of the four strong N_i zones shown in Figure 1, four peaks of upward vertical plasma $\mathbf{E} \times \mathbf{B}$ drifts also have been found by *Kil et al.* [2007]. Thus, the wave number-four longitudinal structure in equinox topside ionospheric N_i may relate to DE3.

[8] The longitude variations of N_i during two solstices show obvious difference with that in equinox. After comparing these longitude distributions in detail, we notice that these longitudinal variations show different features in different longitude range. In the longitude range 150° to 10°, the longitudinal variations of N_i during two solstices show significant anti-correlation with each other. And they both correspond closely to the longitudinal variation of geomagnetic field declination at the dip equator. During two solstices, the summer-to-winter meridional winds could increase N_i at the dip equator through affecting field-aligned plasma transport. Thus, the declination at the dip equator could affect the distributing of N_i through controlling whether the zonal and meridional winds cooperate or oppose one another. During June solstices, as Figure 3 indicates, the field aligned components of daytime westward winds enforce the field-aligned components of the summer-to-winter (north-to-south) meridional winds in the

longitude range150° to 300° where the magnetic declination is positive (eastward) and oppose the field-aligned components of the north-to-south meridional winds in the longitude range 300° to 10° where the magnetic declination is negative (westward). So N_i will increase with declination. During December solstices, the magnetic declination and the zonal wind effect on the meridional winds along the field lines and the longitudinal variation of N_i are opposite to that during June solstices. However, in the longitude range 10° to 150°, the declination is very small and the longitudinal variation of N_i doesn't show notable relativity with the declination. We should notice that the longitudinal variations of N_i between 10° and 150° during two solstices and equinox periods are similar with each other. This may suggest that DE3 also affects the longitude distribution of N_i between 10° and 150° during two solstice periods. So the longitudinal variations of N_i during two solstices may be caused both by the longitudinal variation of declination and DE3.

[9] In conclusion, using the DMSP F13 Satellite equatorial T_e and N_i data acquired from 1995 to 2005, we have studied the longitudinal variations of T_e and N_i in sunset equatorial topside ionosphere. It is shown that. (1) The longitudinal variations of T_e and N_i have obvious seasonal variations. There is an obvious anti-correlation between the longitudinal variation of T_e and N_i, and we speculate that the longitudinal variation of T_e mainly results from the longitudinal variation of N_i, which influences T_e through electron cooling rate. (2) There are wavenumber-four longitudinal structures in equinox topside ionospheric sunset T_e and N_i. They may be the result of the longitudinal variations in the diurnal amplitude of atmospheric tides, associated with DE3 in the daytime E region ionosphere and the corresponding modulation of the daytime zonal electric field. (3) The longitudinal variation of N_i and T_e show notable three peaks longitudinal structure in June solstice and two peaks longitudinal structure in December solstice. These longitudinal variations may be caused by the longitudinal variation of geomagnetic declination (mainly in the longitude range 150° to 10°) and DE3 (mainly in the longitude range 10° to 150°).

[10] **Acknowledgments.** The authors thank Jiuhou Lei from US National Center for Atmospheric Research for his valuable suggestions to the paper. We thank the Center for Space Sciences at University of Texas at Dallas and the US Air Force for providing the DMSP data. The K_p index is taken from the SPIDR web site. This work is supported by the KIP Pilot Project (kzcx2-yw-123) of CAS, National Science Foundation of China (40636032, 40725014), and National important Basic Research Project (2006CB806306).

References

Balan, N., K. I. Oyama, G. J. Bailey, S. Fukao, S. Watanabe, and M. A. Abdu (1997), A plasma temperature anomaly in the equatorial topside ionosphere, *J. Geophys. Res.*, *102*(A4), 7485–7492.

Bilitza, D. (1975), Models for the relationship between electron density and temperature in the upper ionosphere, *J. Atmos. Terr. Phys.*, *37*, 1219–1222.

England, S. L., T. J. Immel, E. Sagawa, S. B. Henderson, M. E. Hagan, S. B. Mende, H. U. Frey, C. M. Swenson, and L. J. Paxton (2006a), Effect of atmospheric tides on the morphology of the quiet time, post-sunset equatorial ionospheric anomaly, *J. Geophys. Res.*, *111*, A10S19, doi:10.1029/2006JA011795.

England, S. L., S. Maus, T. J. Immel, and S. B. Mende (2006b), Longitudinal variation of the *E*-region electric fields caused by atmospheric tides, *Geophys. Res. Lett.*, *33*, L21105, doi:10.1029/2006GL027465.

Hagan, M. E., and J. M. Forbes (2002), Migrating and nonmigrating diurnal tides in the middle and upper atmosphere excited by tropospheric latent heat release, *J. Geophys. Res.*, *107*(D24), 4754, doi:10.1029/2001JD001236.

Hagan, M. E., A. Maute, R. G. Roble, A. D. Richmond, T. J. Immel, and S. L. England (2007), Connections between deep tropical clouds and the Earth's ionosphere, *Geophys. Res. Lett.*, *34*, L20109, doi:10.1029/2007GL030142.

Hartman, W. A., and R. A. Heelis (2007), Longitudinal variations in the equatorial vertical drift in the topside ionosphere, *J. Geophys. Res.*, *112*, A03305, doi:10.1029/2006JA011773.

Henderson, S. B., C. M. Swenson, A. B. Christensen, and L. J. Paxton (2005), Morphology of the equatorial anomaly and equatorial plasma bubbles using image subspace analysis of Global Ultraviolet Imager data, *J. Geophys. Res.*, *110*, A11306, doi:10.1029/2005JA011080.

Immel, T. J., E. Sagawa, S. L. England, S. B. Henderson, M. E. Hagan, S. B. Mende, H. U. Frey, C. M. Swenson, and L. J. Paxton (2006), Control of equatorial ionospheric morphology by atmospheric tides, *Geophys. Res. Lett.*, *33*, L15108, doi:10.1029/2006GL026161.

Kil, H., S.-J. Oh, M. C. Kelley, L. J. Paxton, S. L. England, E. Talaat, K.-W. Min, and S.-Y. Su (2007), Longitudinal structure of the vertical $\mathbf{E} \times \mathbf{B}$ drift and ion density seen from ROCSAT-1, *Geophys. Res. Lett.*, *34*, L14110, doi:10.1029/2007GL030018.

Lei, J., R. G. Roble, W. Wang, B. A. Emery, and S.-R. Zhang (2007), Electron temperature climatology at Millstone Hill and Arecibo, *J. Geophys. Res.*, *112*, A02302, doi:10.1029/2006JA012041.

Lin, C. H., W. Wang, M. E. Hagan, C. C. Hsiao, T. J. Immel, M. L. Hsu, J. Y. Liu, L. J. Paxton, T. W. Fang, and C. H. Liu (2007a), Plausible effect of atmospheric tides on the equatorial ionosphere observed by the FORMOSAT-3/COSMIC: Three-dimensional electron density structures, *Geophys. Res. Lett.*, *34*, L11112, doi:10.1029/2007GL029265.

Lin, C. H., C. C. Hsiao, J. Y. Liu, and C. H. Liu (2007b), Longitudinal structure of the equatorial ionosphere: Time evolution of the four-peaked EIA structure, *J. Geophys. Res.*, *112*, A12305, doi:10.1029/2007JA012455.

Liu, L., B. Zhao, W. Wan, S. Venkartraman, M.-L. Zhang, and X. Yue (2007a), Yearly variations of global plasma densities in the topside ionosphere at middle and low latitudes, *J. Geophys. Res.*, *112*, A07303, doi:10.1029/2007JA012283.

Liu, L., W. Wan, X. Yue, B. Zhao, B. Ning, and M.-L. Zhang (2007b), The dependence of plasma density in the topside ionosphere on the solar activity level, *Ann. Geophys.*, *25*, 1337–1343.

Otsuka, Y., S. Kawamura, N. Balan, S. Fukao, and G. J. Bailey (1998), Plasma temperature variations in the ionosphere over the middle and upper atmosphere radar, *J. Geophys. Res.*, *103*(A9), 20,705–20,713.

Rich, F. J., P. J. Sultan, and W. J. Burke (2003), The 27-day variations of plasma densities and temperatures in the topside ionosphere, *J. Geophys. Res.*, *108*(A7), 1297, doi:10.1029/2002JA009731.

Rishbeth, H., T. E. Van Zandt, and W. B. Hanson (1977), Ion temperature troughs in the equatorial topside ionosphere, *Planet. Space Sci.*, *25*, 629–642.

Sagawa, E., T. J. Immel, H. U. Frey, and S. B. Mende (2005), Longitudinal structure of the equatorial anomaly in the nighttime ionosphere observed by IMAGE/FUV, *J. Geophys. Res.*, *110*, A11302, doi:10.1029/2004JA010848.

Scherliess, L., D. C. Thompson, and R. W. Schunk (2008), Longitudinal variability of low-latitude total electron content: Tidal influences, *J. Geophys. Res.*, *113*, A01311, doi:10.1029/2007JA012480.

Schunk, R. W., and A. F. Nagy (1978), Electron temperatures in the *F* region ionosphere: Theory and observations, *Rev. Geophys.*, *16*(3), 355–399.

Su, Y. Z., K. I. Oyama, G. J. Bailey, S. Fukao, T. Takahashi, and H. Oya (1996), Longitudinal variations of the topside ionosphere at low latitudes: Satellite measurements and mathematical modelings, *J. Geophys. Res.*, *101*(A8), 17,191–17,205.

Venkatraman, S., and R. Heelis (1999a), Longitudinal and seasonal variations in nighttime plasma temperatures in the equatorial topside ionosphere during solar maximum, *J. Geophys. Res.*, *104*(A2), 2603–2611.

Venkatraman, S., and R. Heelis (1999b), Effects of solar activity variations on adiabatic heating and cooling effects in the nighttime equatorial topside ionosphere, *J. Geophys. Res.*, *104*(A8), 17,117–17,126.

Venkatraman, S., and R. Heelis (2000), Interhemispheric plasma flows in the equatorial topside ionosphere, *J. Geophys. Res.*, *105*(A8), 18,457–18,464.

Zhao, B., W. Wan, L. Liu, X. Yue, and S. Venkatraman (2005), Statistical characteristics of the total ion density in the topside ionosphere during the period 1996–2004 using empirical orthogonal function (EOF) analysis, *Ann. Geophys.*, *23*, 3615–3631.

R. A. Heelis, Hanson Center for Space Sciences, University of Texas at Dallas, Richardson, TX 75083-0688, USA.

L. Liu, Z. Ren, W. Wan, Y. Wei, X. Yue, and B. Zhao, Institute of Geology and Geophysics, Chinese Academy of Sciences, Beijing, 100029, China. (wanw@mail.iggcas.ac.cn)